ISSN 2682-681X (Paper), ISSN 2705-4241 (Online) | http://unilorinjoger.com | https://doi.org/10.63745/joger.2025.12.30.017

JOURNAL OF GEOMATICS AND ENVIRONMENTAL RESEARCH
www.unilorinjoger.com

RESEARCH ARTICLE

Geospatial Evaluation of Hydrocarbon Seepage on Vegetation Health in Iba Oku, Uyo Local Government Area of Akwa Ibom State, Nigeria

Ekom Asuquo Etim[1*], Aniekan Effiong Eyoh[1], Bariledum Daniel Nwilag[1]

[1]Department of Geoinformatics and Surveying, University of Uyo, Nigeria

Corresponding email: ekometimgis1111@yahoo.com

Abstract

The study assessed vegetation health in Iba Oku, a hydrocarbon-impacted environment, using multi-temporal normalized difference vegetation index (NDVI) and enhanced vegetation index (EVI) derived from Landsat imagery for 2000, 2012 and 2024. Vegetation stress was evaluated using descriptive statistics, supervised land cover classification, trend direction, and spectral signature assessment. Results revealed a marked decline in vegetation condition between 2000 and 2012 (NDVI and EVI declined by approximately 164% and 500%, respectively), followed by a weak recovery in 2024 (about 156% and 42% by NDVI and EVI, respectively). In 24 years, bare ground increased by 21.81% using NDVI and 22.10% using EVI, while stressed vegetation increased by 24.44% and 25.23% using NDVI and EVI, respectively. Spectral trends and linear projection suggested continued vegetation stress if current environmental pressures persist. The findings demonstrate the value of integrating multiple vegetation indices and spectral information for long-term vegetation health assessment in hydrocarbon-impacted environments and underscore the need for pollution control and sustainable land use planning to support vegetation recovery.

ARTICLE HISTORY
Received: 7th December, 2025
Accepted: 28th December, 2025
Published: 30rd December, 2025

KEYWORDS
Soil Fertility, Spatial Variability, Precision Agriculture, Inverse Distance Weighting (IDW), Trend Interpolation.

Citation: Ekom A. E., Aniekan E. E., Bariledum D. N. (2025). Geospatial Evaluation of Hydrocarbon Seepage on Vegetation Health in Iba Oku, Uyo Local Government Area of Akwa Ibom State, Nigeria, *Journal of Geomatics and Environmental Research, 8(2). Pp192-204*

1. INTRODUCTION

Hydrocarbon seepage occurs when oil and gas migrate from subsurface reservoirs to the Earth's surface through fractures, faults, and permeable geological structures under high pressure (Shi *et al*., 2011; Okereke and Anyadiegwu, 2019; Enoh *et al*., 2022). This process, often described as the chimney effect, is widely recognized as a major environmental concern because of its negative effects on soil quality, vegetation health, and ecosystem stability (Ebele *et al*., 2013). Hydrocarbon seepage is commonly classified as active or passive. Active seepage involves continuous migration of oil and gas to the surface and is often detectable through geophysical anomalies. Passive seepage refers to areas where hydrocarbons are present but migrate slowly or intermittently, producing subtle surface expressions. Both forms can induce vegetation stress that is detectable through changes in spectral reflectance (Abrams, 2005; Schumacher, 2002). In seepage-affected environments, hydrocarbons alter soil chemistry and reduce oxygen availability within the root zone. These changes restrict water and nutrient uptake by plants and lead to chlorosis, reduced growth, and eventual vegetation decline (Schumacher, 2001; David *et al*., 2017; Enoh *et al*., 2022). Prolonged seepage can also result in the loss of fertile soils, contamination of surface and groundwater, and disruption of local ecosystems (Aghalino, 2000; Alrowais *et al*., 2023).

Remote sensing and geographic information system provides effective, non-invasive tools for monitoring vegetation stress associatedwith hydrocarbon contamination. Unlike conventional geochemical and geophysical methods, remote sensing offers broad spatial coverage, reduced cost, and the ability to monitor environmental change over long time periods (Lyon *et al*., 1998; Okereke and Anyadiegwu, 2019). Vegetation indices derived from satellite imagery are particularly useful for detecting stress-related changes in plant condition.

The Normalized Difference Vegetation Index (NDVI) has been widely applied in oil spill and seepage studies due to its effectiveness in distinguishing healthy vegetation from stressed vegetation and bare surfaces (Schumacher, 2001; Wilton, 2021). NDVI responds strongly to reductions in chlorophyll content and near-infrared reflectance caused by hydrocarbon-induced stress (Jamaludin *et al*., 2015). However, NDVI alone may be limited in areas with dense vegetation or atmospheric interference. The Enhanced Vegetation Index (EVI) addresses some of these limitations by incorporating the blue band to reduce atmospheric influences and improve sensitivity in high-biomass regions (Huete *et al*., 2002).

Although numerous studies in the Niger Delta have relied predominantly on NDVI for assessing vegetation impacts of oil pollution (Okereke and Enoh, 2016; Adamu *et al*., 2018; Erebi and Davidson, 2023; Afifi, 2015; Adamu *et al*., 2021), comparatively few have integrated EVI (Adamu *et al*., 2015)and spectral signature analysis within a multi-temporal framework. This study addresses this gap by combining NDVI, EVI, supervised classification, and spectral analysis to provide a robust, spatially explicit assessment of vegetation response to hydrocarbon seepage in Iba Oku, Akwa Ibom State, Nigeria.

2. MATERIALS AND METHODS

This study used geospatial methods that combine remote sensing and geographic information systems to examine how hydrocarbon seepage affects vegetation health in Iba Oku. The study followed three main steps: data collection, image pre-processing and data analysis. These steps were carefully applied to ensure accurate, consistent and reliable results across all time periods studied. This approach enabled the comparison of vegetation conditions before, during, and after the seepage occurred in the study area.

2.1 Study area

The study was conducted in Iba Oku, located within the Uyo Local Government Area of Akwa Ibom State, Nigeria (Fig. 1). Iba Oku lies within the Niger Delta region and forms part of the Oku clan in Uyo. The area is situated between latitudes 5° 03' – 5° 05' N and longitudes 7° 55' – 7° 57' E, covering approximately 90.2 km2. Land use in the area is predominantly agricultural, with scattered built-up areas, water bodies, sand quarry sites and forested zones. The terrain is generally flat and underlain by coastal plain sediments. The climate is characterized by a warm, humid wet season and a hot, dry season. According to the 2006 national census, Iba Oku has an estimated population of about 2,580 people.

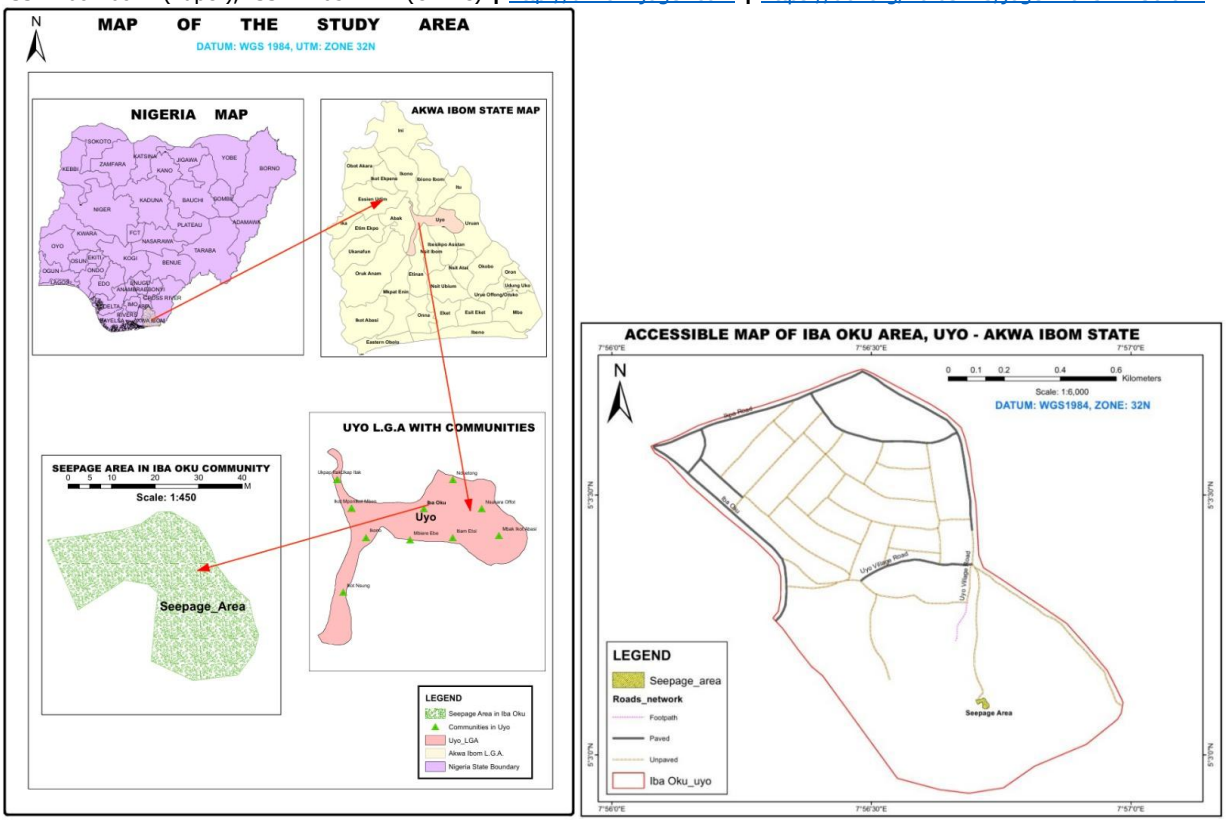

Figure 1. Map of the Study Area

2.2 Data Acquisition

Both primary and secondary data were used. Primary data included Global Navigation Satellite System (GNSS) coordinates of observed hydrocarbon seepage locations and field photographs collected during site visits. GNSS measurements were acquired with sub-meter positional accuracy. Secondary data consisted of multi-temporal Landsat imagery: Landsat 7 ETM+ (2000), Landsat 8 OLI/TIRS (2012), and Landsat 9 OLI/TIRS-2 (2024), obtained from the United States Geological Survey (USGS). Additional data included Google Earth imagery and relevant literature. Landsat datasets were selected due to their consistent spectral characteristics, 30 m spatial resolution, and suitability for vegetation monitoring over long temporal scales. Landsat 7 has eight spectral bands (including a panchromatic band) with 30m resolution for multispectral bands and 15m for panchromatic. Landsat 8 captures eleven spectral bands, including new coastal aerosol and cirrus bands, with 30m resolution (15m for panchromatic), and Landsat 9 offers similar spectral and spatial characteristics as Landsat 8 but with improved radiometric calibration. Images were acquired during periods of minimal cloud cover to ensure data quality. For this study, Landsat images acquired on 20th December 2000, 17th January 2012 and 23rd December 2024 were used. A Shuttle Radar Topographic Mission (SRTM) digital elevation model was used to support spatial referencing

Table 1. Data Acquired for the Study and Sources

S/N	Data	Type	Source	Path/Row	Format	Scale/Resolution	Date
1	Landsat 7 ETM+	Secondary	USGS	188/57	Digital	30m	2000
2	Landsat 8 TIRS/OLI	Secondary	USGS	188/57	Digital	30m	2012
3	Landsat 9 TIRS/OLI	Secondary	USGS	188/57	Digital	30m	2024
4	Google Earth Image	Secondary	Google Earth		Digital	15m	2024
5	GNSS Coordinates	Primary	Field Work		Digital	±5cm	2024
6	Pictures	Primary	Field Work		Digital	50MP	2024

Figure 2. Seepage Area, (Iba Oku, Uyo)

2.3 Image Pre-processing

Landsat images used in this study were level-1 terrain-corrected (L1T) data. Although L1T data undergo systematic radiometric calibration, geometric correction, and terrain correction, these processes are limited to sensor-level and geometric adjustments. Atmospheric effects remain uncorrected, and additional pre-processing such as atmospheric correction, is required before the data can be reliably used for quantitative surface reflectance analysis and multi-temporal change detection. Atmospheric correction refers to the process of adjusting the recorded satellite imagery to account for atmospheric effects and obtain accurate measurements of the Earth's surface. The equations for atmospheric correction of Landsat images from Digital Number (DN) to Top of Atmosphere (TOA) reflectance using reflectance re-scaling coefficients from the Landsat metadata file are provided in Equations (1) and (2).

TOA reflectance without correction for solar angle (ρλ') can be calculated using Equation (1):

$$p\lambda = Mp.Qcal + Ap \quad \text{Equation (1)}$$

Where ρλ represents TOA planetary reflectance, Mp is the band-specific multiplicative re-scaling factor, Aρ is the band-specific additive re-scaling factor, and Qcal refers to the quantized and calibrated standard product pixel values (DN).

TOA reflectance corrected for the sun angle can be calculated using Equation (2):

$$p\lambda' = (p\lambda)/\cos(\theta sz) = (p\lambda)/\cos(\theta se) \quad \text{Equation (2)}$$

Where θsz represents the solar zenith angle, while θse represents the solar elevation angle.

In this study, the Landsat images were corrected atmospherically using the fast line-of-sight atmospheric analysis of hypercubes (FLAASH) in ENVI.

2.4 Computation of Vegetation Indices

Vegetation health was assessed using the Normalized Difference Vegetation Index (NDVI) and the Enhanced Vegetation Index (EVI) for the three years. NDVI was computed using read and near-infrared reflectance to indicate vegetation vigour and photosynthetic activity. EVI incorporated the blue band to improve sensitivity in areas with dense vegetation and atmospheric interference. Both indices served as indicators of vegetation stress potentially induced by hydrocarbon seepage.

NDVI is expressed as shown in Equation (3).

$$NDVI = \frac{NIR\text{-}R}{NIR+R} \quad \text{Equation (3)}$$

Where NIR (Near-Infrared) and R (Red)

For Landsat 7, NDVI was computed using Bands 4 (NIR) and 3 (Red), while for Landsat 8 and 9, NDVI was computed using Bands 5 (NIR) and 4 (Red).

EVI is calculated as shown in Equation (4).

$$EVI = \frac{2.5(NIR\text{-}R)}{(NIR+6R\text{-}7.5B+1)} \quad \text{Equation (4)}$$

Where NIR (Near-Infrared), R (Red) and B (Blue)

For Landsat 7, EVI was computed using Bands 4 (NIR), 3 (Red) and 1 (Blue), while for Landsat 8 and 9, EVI was computed using Bands 5 (NIR), 4 (Red), and 2 (Blue).

NDVI and EVI are designed to standardize vegetation index values to a range between -1 and +1, providing a measure of the health of vegetation within a pixel. Values between -1 and 0.3 indicate poor vegetation status; 0.3 to 0.5 indicate normal vegetation conditions, and 0.5 to 1.0 indicate a healthy condition.

2.5 Land-Cover Classification

Supervised land-cover classification was performed using the Maximum Likelihood Classification algorithm in ArcMap. Three classes were defined: unstressed vegetation, stressed vegetation, and bare ground. Training samples representing stressed vegetation, unstressed vegetation, and bare land were selected based on spectral characteristics and visual interpretation. Spectral signatures were generated for each class, and pixels were assigned based on probability density functions. Classified outputs were converted to vector format to quantify areal coverage. Check Table 8 for the classification statistics.

2.6 Spectral Signature Analysis and Simulation

Spectral signatures for stressed and unstressed vegetation were extracted for 2000, 2012 and 2024. Changes in reflectance, particularly in the read and near-infrared regions were analyzed to assess vegetation response to seepage. A spectral projection for 2036 was generated using linear regression and python based on temporal reflectance trends (using the data in Table 2). The simulation provided insight into potential future vegetation conditions if seepage persists.

Table 2. Input Data for Simulation

Year	450 nm	550 nm	650 nm	700 nm	850 nm	950 nm
2000	0.07	0.1	0.08	0.12	0.26	0.18
2012	0.09	0.12	0.1	0.13	0.22	0.15
2024	0.13	0.16	0.14	0.17	0.18	0.12

Sample Python code used for the prediction is as follows:

```
Wavelengths = [450, 550, 650, 700, 850, 950]
reflectance_2000 = [0.07, 0.10, 0.08, 0.12, 0.26, 0.18]
reflectance_2012 = [0.09, 0.12, 0.10, 0.13, 0.22, 0.15]
reflectance_2024 = [0.13, 0.16, 0.14, 0.17, 0.18, 0.12]

Years = np.array([[2000], [2012], [2024]])
reflectance_all = np.array([reflectance_2000, reflectance_2012, reflectance_2024])

predicted_2036 = [ ]
for i in range(len(wavelengths)):
    y = reflectance_all[:, i]
    model = LinearRegression().fit(years, y)
    prediction = model.predict([[2036]])
    predicted_2036.append(prediction[0])
```

3. RESULTS

3.1 NDVI Analysis of Vegetation Health and Stress (2000 – 2024)

The NDVI statistics in Table 3 show a clear decline in vegetation health in the study area over the study period. In 2000, the mean NDVI value was 0.14, which indicates sparse but functional vegetation cover with a maximum NDVI of 0.45. In 2012, the mean and maximum NDVI dropped sharply to -0.09 and 0.38, respectively, indicating severe vegetation stress. By 2024, the mean NDVI slightly increased to 0.05, but this value remained low, indicating weak vegetation recovery as shown by the continuous decline in the maximum NDVI for 2024. These results signify a progressive decline in vegetation biomass and greenness between 2000 and 2024. The NDVI classification results in Table 4 confirm this trend. This pattern shows continuous vegetation degradation and land exposure. Unstressed vegetation decreased from 51.36% in 2000 to 39.74% in 2024. At the same time, bare ground expanded from 10.59% to 12.90%. It's observed

that a slight increment in the NDVI in 2024 (Table 3) causes a corresponding decrease in the amount of stressed vegetation and bare ground by 0.03% and 0.05%, respectively (Table 4). This confirms that NDVI is sensitive to chlorophyll content and vegetation density.

Table 3. Descriptive statistics for NDVI values during 2000 – 2024

Year	Min	Max	Mean	Standard deviation
2000	-0.19	0.45	0.14	0.05
2012	-0.20	0.38	-0.09	0.02
2024	-0.22	0.35	0.05	0.01

Table 4: NDVI Vegetation Stress classification results of Iba Oku

Vegetation Health	2000		2012		2024	
	Area (km^2)	%	Area (km^2)	%	Area (km^2)	%
Bare ground	9.55	10.59	11.68	12.95	11.64	12.90
Stressed	34.32	38.05	42.68	47.32	42.71	47.35
Unstressed	46.33	51.36	35.84	39.73	35.85	39.74
Total	**90.2**	**100**	**90.2**	**100**	**90.2**	**100**

NDVI maps for the study periods (Figure 3) clearly depict these temporal differences, highlighting visible reductions in healthy vegetation in the study area.

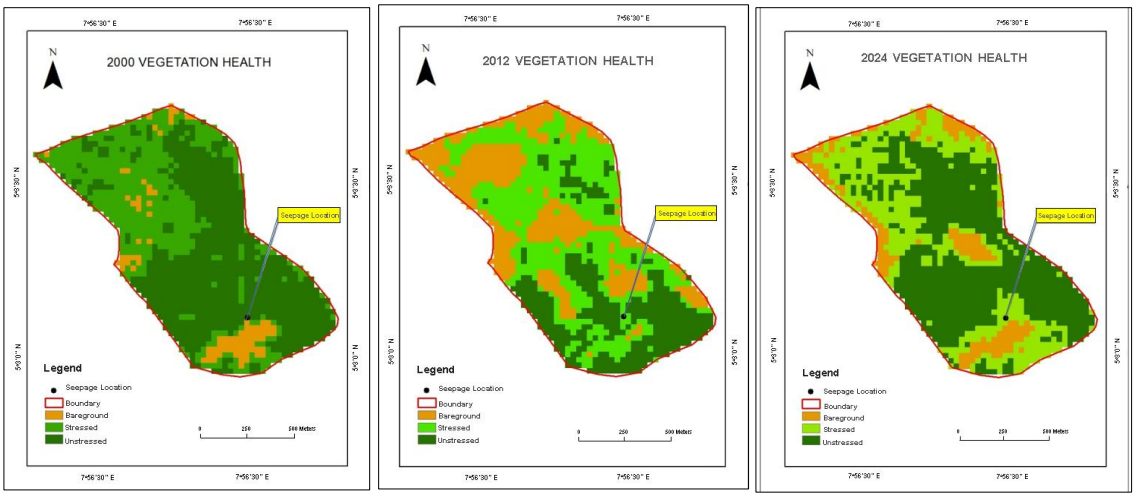

Figure 3. NDVI vegetation stress level in 2000, 2012, and 2024

3.2 EVI Analysis of Vegetation Health (2000 – 2024)

Table 5 shows the descriptive statistics for EVI. In 2000, the maximum and mean EVI were 0.12 and 0.15, respectively, indicating relatively good vegetation vigour. In 2012, the maximum and mean EVI dropped sharply to -0.51 and -0.60, showing severe vegetation stress. In 2024, while the mean EVI improved slightly to -0.35, the maximum EVI yet dropped to -0.48, indicating unhealthy vegetation conditions. In Table 7, the abstract EVI index values are translated into meaningful vegetation stress classes. Unstressed vegetation declined from 51.21% in 2000 to 39.25% in 2024, while stressed vegetation increased to over 47%. Bare ground increased gradually from 11.22% in 2000 to 13.70% in 2024. EVI values measure substantial vegetation degradation rather than temporary seasonal effects. This explains why a temporary increase in the mean EVI in 2024 in Table 5 didn't produce any corresponding effect on the vegetation classes in Table 6 as experienced in the case of NDVI. The negative EVI values suggest severe structural degradation of vegetation consistent with hydrocarbon stress since it is more sensitive to canopy structure and biomass.

Table 5. Descriptive statistics for EVI values during 2000 – 2024.

Year	Min	Max	Mean	Standard deviation
2000	-0.69	0.12	0.15	0.13
2012	-0.78	-0.51	-0.60	0.05
2024	-0.24	-0.48	-0.35	0.03

Table 6. EVI Vegetation Stress classification results of Iba Oku

Vegetation Health	**2000**		**2012**		**2024**	
	Area (km^2)	%	Area (km^2)	%	Area (km^2)	%
Bare ground	10.12	11.22	11.86	13.15	12.36	13.70
Stressed	33.89	37.57	42.08	46.65	42.44	47.05
Unstressed	46.19	51.21	36.26	40.20	35.40	39.25
Total	**90.2**	**100**	**90.2**	**100**	**90.2**	**100**

Spatial EVI maps for the study periods (Figure 4) clearly depict vegetation degradation in the study area.

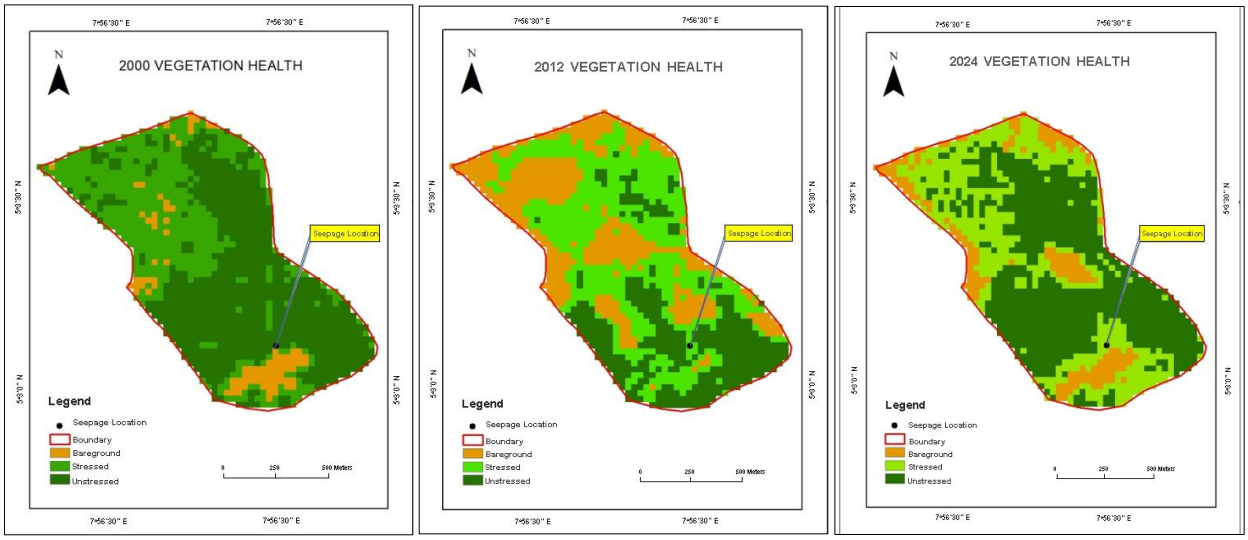

Figure 4: EVI vegetation stress level in 2000, 2012 and 2024

3.3 Relationship between NDVI and EVI (2000 – 2024)

The Pearson correlation coefficient between NDVI and EVI across all three study years 0.95 (Table 7). This indicates a very strong positive relationship between both indices. This also indicates that both indices respond similarly to vegetation changes in the study area, especially in 2012 during the extreme vegetation stress. NDVI and EVI exhibit similar temporal behaviour, confirming their strong positive relationship. However, EVI shows greater sensitivity to vegetation degradation during periods of severe stress. This shows its suitability for assessing structurally damaged vegetation in hydrocarbon-impacted environments (Fig. 5). In Figure 6, the percentage distribution of vegetation health classes derived from both NDVI and EVI are compared, and the progressive loss of healthy vegetation cover for 24 years due to hydrocarbon toxicity and land degradation is presented. The similarity in their percentage patterns shows that the observed degradation is real and systematic, not an artefact of one index.

Table 7: Pearson correlation

	NDVI	*EVI*
Mean	0.033	-0.267
Variance	0.013	0.146
Observations	3	3
Pearson Correlation	0.950	

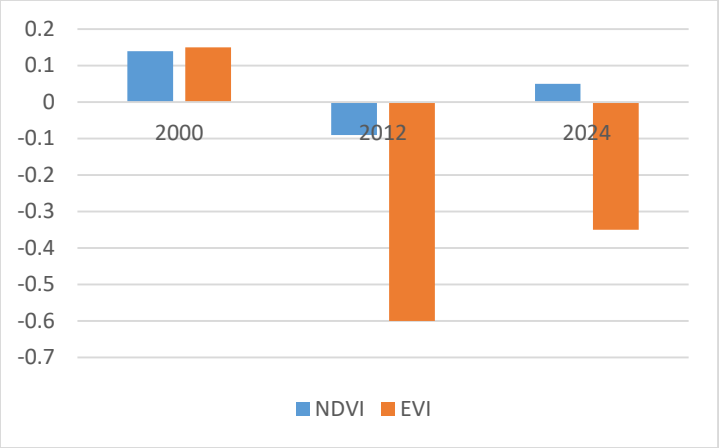

Figure 5. Mean NDVI vs. mean EVI for the study periods.

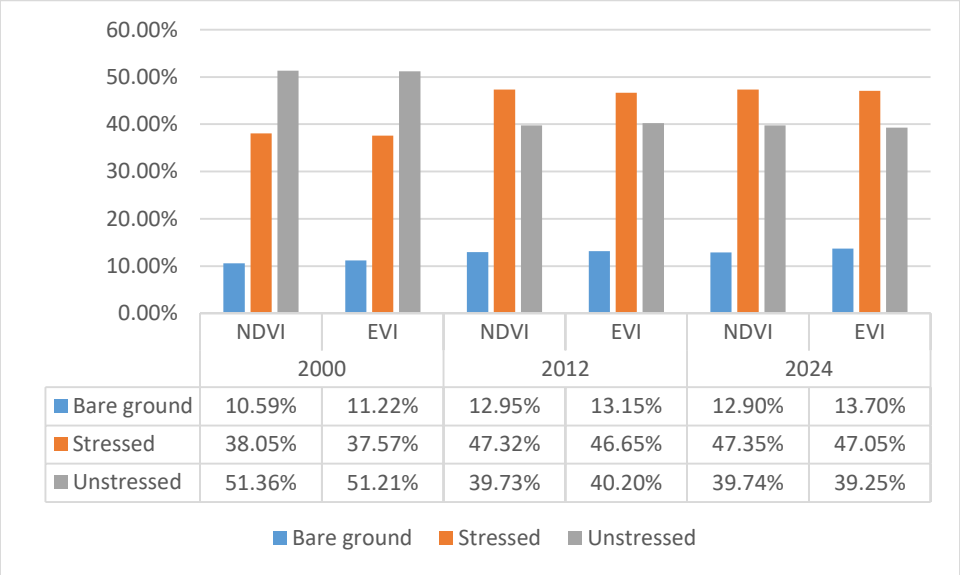

	NDVI 2000	EVI 2000	NDVI 2012	EVI 2012	NDVI 2024	EVI 2024
Bare ground	10.59%	11.22%	12.95%	13.15%	12.90%	13.70%
Stressed	38.05%	37.57%	47.32%	46.65%	47.35%	47.05%
Unstressed	51.36%	51.21%	39.73%	40.20%	39.74%	39.25%

Figure 6. Percentage change in vegetation classes for the study periods

3.4 Spectral Signature Analysis and Prediction for 2036

The spectral signature (Figure 7) shows that unstressed vegetation consistently had higher reflectance in the near-infrared bands (850–950 nm) than stressed vegetation. Healthy vegetation reflects strongly in the near-infrared due to intact leaf structure. The reduced reflectance observed in stressed vegetation indicates damage to leaf cells and reduced chlorophyll content. In 2000, reflectance patterns indicated healthy vegetation, with no significant evidence of stress, consistent with the absence of seepage during this period. In 2012, both stressed and unstressed vegetation showed reduced reflectance across wavelengths, with stressed vegetation displaying markedly lower near-infrared (NIR) reflectance, signalling vegetation degradation. In 2024, reflectance values for stressed vegetation showed a drastic decline across all wavelengths, with pronounced reductions in NIR reflectance, indicating severe structural and biochemical deterioration attributable to hydrocarbon seepage.

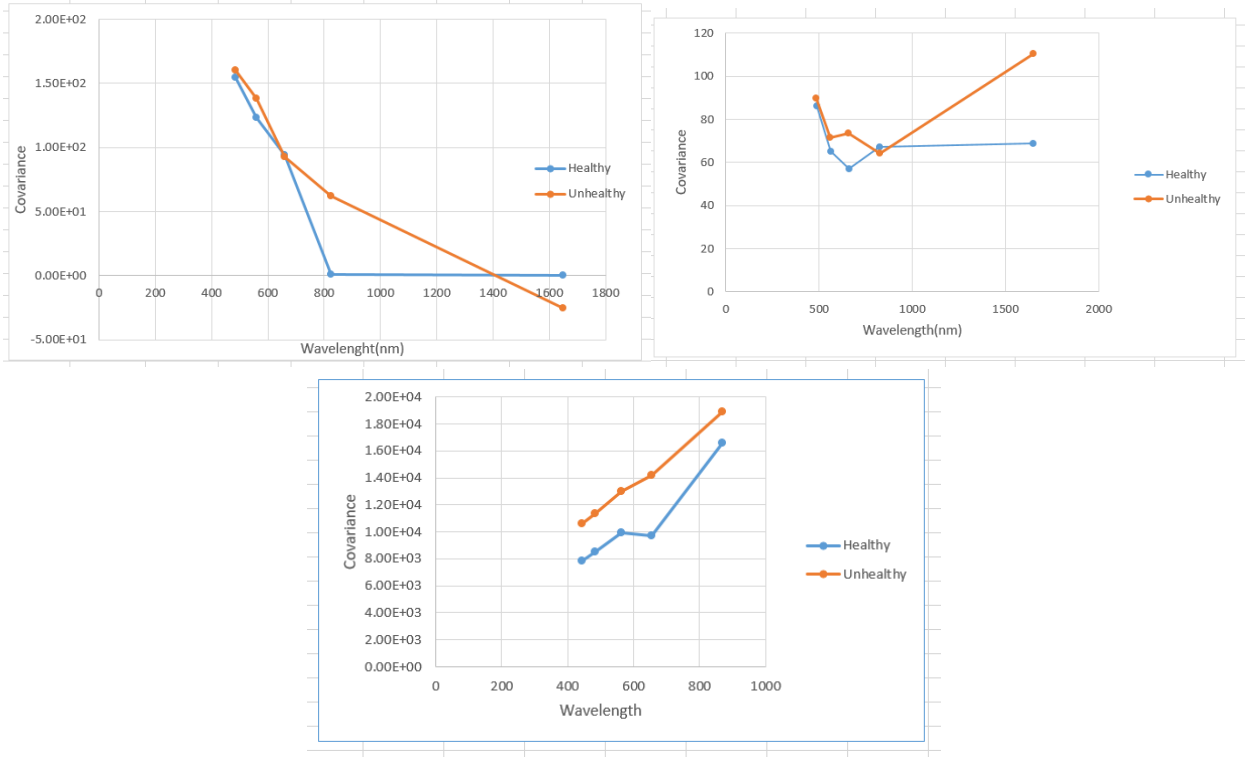

Figure 7. Spectral Signature of stressed and unstressed vegetation in 2000, 2012 and 2024

The linear regression prediction for 2036 shows further reduction in near-infrared reflectance (Fig. 8). This suggests that vegetation stress may intensify if current environmental conditions continue. Reduced near-infrared reflectance is a recognized indicator of long-term vegetation stress linked to soil contamination and ecological disturbance.

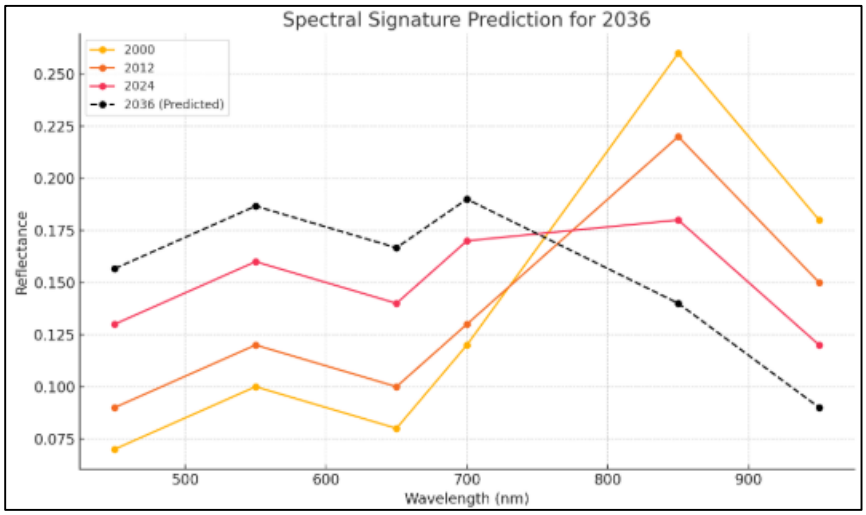

Figure 8. Spectral Signature Prediction for 2036

3.5 Classification Accuracy

The accuracy assessment shows producers' and users' accuracies above 80% across all years (Table 8). This confirms that the observed vegetation changes are reliable and not due to classification errors. High classification accuracy strengthens confidence in the detected trends. The overall classified accuracy for 2000, 2012, and 2024 were 80.6%, 82.6% and 85.7%, respectively, while the Kappa statistics were 0.8, 0.8, and 0.9 for 2000, 2012, and 2024, respectively.

Table 8. Accuracy Assessment for Land-Cover Classifications using MLC algorithm

Vegetation Stress	Number of correctly classified test pixels	Number of incorrectly classified test pixels	Total Number of test pixels	Producer's Accuracy or class Accuracy (%)	User's Accuracy (%)
2000 Classification					
Bare-ground	50	1	51	100	98
Unstressed Vegetation	46	3	49	98	94
Stressed Vegetation	46	9	55	92	84
2012 Classification					
Bare-ground	40	1	41	100	98
Unstressed vegetation	41	0	41	98	100
Stressed Vegetation	49	1	50	98	98
2024 Classification					
Bare-ground	50	1	51	100	98
Unstressed Vegetation	40	1	39	98	100
Stressed Vegetation	25	1	26	100	100

4. DISCUSSION

The results demonstrate a long-term decline in vegetation health in Iba Oku, with the most severe degradation occurring between 2000 and 2012 (the mean NDVI and EVI declined sharply by approximately 164% and 500%, respectively). The limited recovery observed by 2024 (about 156% and 42% by NDVI and EVI respectively) suggests that vegetation structure and biomass remain compromised. Despite the weak recovery in 2024, the NDVI and EVI values remained lower than baseline conditions recorded in 2000. Using NDVI, bare ground increased by 21.81% while stressed vegetation increased by 24.44% between 2000 and 2024. Conversely, bare ground and stressed vegetation increased by 22.10% and 25.23% respectively between 2000 and 2024 using EVI. EVI indicates extreme degradation than NDVI due to its sensitivity to canopy loss and biomass reduction. Also, recovery is weaker in EVI than NDVI implying that vegetation structure did not recover as much as greenness. Both NDVI and EVI exhibited negative slope which indicates a consistent decline in vegetation condition across the study area for 24 years. These trends align with previous studies in the Niger Delta that reported declining NDVI and other vegetation indices in areas affected by oil pollution and environmental disturbance (Adebangbe, 2025, Kuta *et al*., 2025).

Spectral signatures show that healthy vegetation reflected more near-infrared light than stressed vegetation. The predicted reduction in near-infrared reflectance for 2036 suggests that vegetation stress will continue if current environmental pressures persist. Reduced near-infrared reflectance is a known indicator of deteriorating vegetation condition due to soil contamination and ecological stress. These results match findings from comparable research in the Niger Delta where vegetation indices have been used to quantify oil spill impacts and broader degradation processes (Asadzadeh and de Souza Filho 2017; Adebangbe, 2025).

Hydrocarbon seepage and oil spills are well-established drivers of vegetation degradation in the Niger Delta (Adebangbe, 2025, Mohamadi *et al*., 2015, Erebi and Davidson, 2023, Akpoghelie, 2021, Adamu *et al*., 2021). While hydrocarbon seepage is a key driver of vegetation stress, other factors such as agricultural intensification, land-use change, and soil degradation likely contribute synergistically. Soil degradation from continuous cropping and monoculture has been linked to loss of vegetation cover and soil fertility in Niger Delta soils. Although specific hydrocarbon contamination data were not measured in this study, degraded soil quality from both agricultural pressure and hydrocarbon seepage can synergistically suppress vegetation growth. Land use changes also affect vegetation health. Expansion of farming, bush burning, and shortened fallow periods degrade soil quality and reduce vegetation cover. These practices expose soil and increase the spatial extent of bare ground. Studies in the Niger Delta and nearby regions highlighted

that agricultural expansion and land conversion influence vegetation cover and can exacerbate stress detected by NDVI and EVI ((Phil-Eze *et al*., 2021, Agumagu *et al*., 2025).

5. CONCLUSION

This study evaluated vegetation health in Iba Oku, a hydrocarbon-impacted area using multi-temporal NDVI and EVI between 2000 and 2024. The results revealed a pronounced decline in vegetation condition with severe degradation observed between 2000 and 2012 and only limited recovery in 2024. Both vegetation indices showed consistent temporal patterns confirming their reliability for monitoring vegetation health. However, EVI exhibited stronger sensitivity to degradation, indicating substantial loss of vegetation structure and biomass within the study period. Vegetation stress classification further demonstrated a progressive increase in stressed vegetation and bare ground, accompanied by a marked reduction in healthy vegetation cover. Spectral signature analysis supported these findings showing declining near-infrared reflectance consistence with stressed and degraded vegetation. The observed vegetation degradation reflects the combined effects of hydrocarbon seepage, land use change, and agricultural disturbance within the study area. The study highlights the effectiveness of integrating multiple vegetation indices and spectral information for assessing long-term ecological change in oil-producing regions. The findings underscore the need for improved pollution control and sustainable land-use practices to support vegetation recovery and healthy environment in the Niger Delta.

REFERENCE

Abrams M.A. 2005, 'Significance of hydrocarbon seepage relative to petroleum generation and entrapment', Marine Petroleum Geology, 22:457 – 477.

Adamu, B., Tansey, K. & Ogutu, B. 2015, 'Using vegetation spectral indices to detect oil pollution in the Niger Delta', Remote Sensing Letters, 6:2, 145-154.

Adamu, B., Tansey, K. & Ogutu, B. 2018, 'Remote sensing for detection and monitoring of vegetation affected by oil spills', International Journal of Remote Sensing, 39(11): 3628-3645

Adamu, U. W., Yeboah, E. & Sarfo, I. 2021, 'Assessment of Oil Spillage Impact on Vegetation in South-Western Niger Delta, Nigeria', Journal of Geography, Environment and Earth Science International, 25(9): 31-45.

Adebangbe, S. A., Dixon, D. P., & Barrett, B. 2025, 'Evaluating contaminated land and the environmental impact of oil spills in the Niger Delta region: a remote sensing-based approach', Environmental Monitoring and Assessment, 197(10), 1149.

Afifi, B. M. I. 2015, 'Assessment of Oil Spill Impact on Nigeria's Rivers State Vegetation using GIS and Remote Sensing Techniques', PhD Thesis, Faculty of Information Engineering, China University of Geosciences Wuhan, China.

Aghalino, S. O. 2000, 'Petroleum Exploitation and Agitation for Compensation by Oil Producing Communities in Nigeria', Geo Studies Forum, Issue I & II, pp. 11 – 20.

Agumagu, O. O., Marchant, R. and Stringer, L. C. 2025, 'Land Use and Land Cover Change Dynamics in the Niger Delta Region of Nigeria from 1986 to 2024', Land 2025, 14(4), 765.

Akpoghelie, O. J., Igbuku, U. A. & Osharechiren, E. 'Oil spill and the Effects on the Niger Delta Vegetation: A Review', Nigerian Research Journal of Chemical Sciences, 9(1): 1 – 12.

Almalki, R., Khaki, M., Saco, P. M., & Rodriguez, J. F. 2022, 'Monitoring and mapping vegetation cover changes in Arid and Semi-Arid Areas using Remote Sensing Technology: A review', Remote Sensing, 14(20), 5143.

Alrowais, R., Alwushayh, B., Bashir, M. T., Nasef, B. M., Ghazy, A., & Elkamhawy, E. 2023, 'Modelling and analysis of cutoff wall performance beneath water structures by Feed-Forward Neural Network (FFNN)', Water, 15(21), 3870.

Asadzadeh, S. & de Souza Filho, C.R. 2017, 'Spectral Remote Sensing for Onshore Seepage Characterization: A Critical Overview', Earth-Science Reviews, 168, 48-72.

Brown, A. 2000, 'Evaluation of possible gas micro-seepage mechanisms', AAPG Bulletin, 84:1775 – 1789.

David, M. B., Matthijs, B., Richard G., and James, J. B. 2017, 'Heavy hydrocarbon fate and transport in the environment', Quarterly Journal of Engineering Geology and Hydrogeology, 50: pp 333 - 346

Ebele, J. E. 2013, 'Remote Sensing Technology: An indispensable tool for combating oil Pollution via plant stress response', International Journal of Engineering Research & Technology (JERT) Vol. 2 Issue 3, pp 1 – 12

El-Mahdy, M. T., Hamed, H. A., Mohamed, H. I., & Dawood, M. F. 2024, 'Rhizomicrobiome as potential agents used against polyaromatic hydrocarbons contaminated soils for plants' pp. 449–471, In

Joginder Singh, Vikas Sharma (eds) Rhizomicrobiome in Sustainable Agriculture and Environment, Academic Press, London.

Enoh, M. A., Njoku, R. E> & Igbokwe, E. C. 2021, 'Geospatial Interpretation of Onshore Hydrocarbon Micro–Seepage Induced Alterations in Soils and Sediments by Spectral Enhancement Techniques', International Journal of Design & Nature and Ecodynamics, 16(3): 307 – 313.

Enoh, M. A., Okeke, F. I. & Okereke, C. A. 2019, 'Geospatial Risk Assessment and Modelling of Natural Hydrocarbon Seepage in Ugwueme ', African Journal of Environment and Natural Science Research, 2(3): 62-70

Enoh, M. A., Okeke, U. C., & Barinua, N. Y. 2020, 'Modelling and Delineation of Hydrocarbon Micro - Seepage Prone Zones on Soil and Sediment in Ugwueme, South Eastern Nigeria with Soil Adjustment Vegetation Index (SAVI)', International Journal of Plant & Soil Science, 13 – 33.

Enoh, M., Onwuzuligbo, C., & Narinu, N. 2022, 'Stimulating the impact of hydrocarbon micro-seepage on vegetation in Ugwueme, South-Eastern Nigeria from 1996 to 2030, based on the Leaf Area Index and Markov Chain Model', Engineering Proceedings, 31(1), 47.

Erebi, J. L. & Davidson, E. E. 2023, 'Application of Vegetation Indices for Detection and Monitoring Oil Spills in Ahoada West Local Government Area of Rivers State, Nigeria', Journal of Geographical Research, 6(3): 29- 41.

Erebi, J. L., & Davidson, E. E. 2023, 'Application of vegetation indices for detection and monitoring oil spills in Ahoada West Local Government area of Rivers State, Nigeria', Journal of Geographical Research, 6(3), 29–41.

Eyoh, A., and Ubom, O. 2016, 'Spatio- Temporal Analysis of Land Use/Land Cover Change Trend of Akwa Ibom State, Nigeria from 1986-2016 using Remote Sensing and GIS', International Journal of Science and Research (IJSR): 6 – 14.

Iloabuchi, N. E., Omokaro, G. O. & Agbede, O. E. 2024, 'Oil Spillage Monitoring in Nigeria and the Role of Remote Sensing - An Overview', Am. J. Environ. Clim. 3(1): 78-87.

Jamaludin, M. I., Matori, A. N., and Myint, K. C. 2015, 'Application of NIR to determine effects of hydrocarbon microseepage in oil palm vegetation stress', Proceeding of the 2015 International Conference on Space Science and Communication (IconSpace), 10 – 12 August, 2015, Langkawi, Malaysia.

Küçük, H. M., Dondurur, D., Özel, Ö., & Cifci, G. 2015, 'Acoustic investigations of gas and gas hydrate formations, offshore Southwestern Black Sea', American Geophysical Union, Fall Meeting 2015,

Kuta, A. A., Grebby, S., & Boyd, D. S. 2025, 'Remote monitoring of the impact of oil spills on vegetation in the Niger Delta, Nigeria', Applied Sciences, 15(1), 338.

Kuta, A. A., Grebby, S., & Boyd, D. S. 2025, 'Remote monitoring of the impact of oil spills on vegetation in the Niger Delta, Nigeria', Applied Sciences, 15(1), 338.

Li, A., Yin, S., Li, N., & Shi, C. 2025, 'Comprehensive analysis of the driving forces behind NDVI variability in China under climate change conditions and future scenario projections', Atmosphere, 16(6), 738.

Lyon, J. G., Yuan, D., Lunetta, R. S., & Elvidge, C. D. 1998, 'A change detection experiment using vegetation indices', Photogrammetric Engineering & Remote Sensing 64(2)

Mohamadi, B., Liu, F. & Xie, Z. 2016, 'Oil Spill Influence on Vegetation in Nigeria and Its Determinants', Pol. J. Environ. Stud. Vol. 25, No. 6, 2533-2540.

Mohamadi, B., Xie, Z. & Liu, F. 2015, 'GIS Based Oil Spill Risk Assessment Model for the Niger Delta's Vegetation', Nature Environment and Pollution Technology, 14(3):545-552.

National Population Commission (NPC) (2006) Nigeria National Census: Population Distribution by Sex, State, LGAs and Senatorial District: 2006 Census Priority Tables (Vol. 3).

http://www.population.gov.ng/index.php/publication/140-popn-distri-by-sex-state-jgas-and-senatorial-distr-2006. Retrieved 1st December, 2025.

Nila, M. U. S., Bobrowski, M., & Schickhoff, U. 2025, 'Growing season normalized difference Vegetation index in the Nepal Himalaya and adjacent areas, 2000–2019: sensitivity to climate change and terrain factors', Land, 14(4), 749.

Noomen, M. F. 2007, 'Hyperspectral reflectance of vegetation affected by underground hydrocarbon seepage', Ph.D thesis, ITC.

Okeke, F. I. & Enoh, M. A. 2016, 'Analysing the Effect of Hydrocarbon Seepage on Vegetation in Ugwueme Town, Awgu Local Government Area of Enugu State using Normalized Differencing Vegetation Index (NDVI) Threshold Classification Method', International Journal of Multidisciplinary Research and Modern Education (IJMRME), 2(2): 446 – 454.

Okereke, C. A., & Anyadiegwu, P. C. 2019, 'Mapping and analysis of vegetation spectral reflectance in oil and gas seepage polluted zones using six vegetation indices' Journal of Environment and Earth Science, 10(10):20 – 28.

Ozigis, M. 2020, 'Detection and mapping of terrestrial oil spill impact using remote sensing data in combination with machine learning methods: a case site within the Niger Delta Region of Nigeria', Environmental Pollution, 256:113360

Phil-Eze, P. O., Elekwachi, W., Bosco-Abiahu, L. C., Collins, H. W., Muktar, A., Omobolaji, O. A., & Eze, I. C. 2021, 'Vegetation Change Detection in the Niger Delta Region of Nigeria using Remote Sensing and GIS Techniques from 2000 to 2020', Asian Journal of Environment & Ecology, 181–188.

Schumacher, D. 2001, 'Petroleum exploration in environmentally sensitive areas: Opportunities for non-invasive geochemical and remote sensing methods', pp. 12 15.

Schumacher, D. 2002, 'Hydrocarbons Geochemical Exploration for Petroleum', AAPG, Memoir 66, pp 184-204.

Serrano, J., Shahidian, S., Paixão, L., Da Silva, J. M., & Paniágua, L. L. 2024, 'Pasture Quality Assessment through NDVI Obtained by Remote Sensing: A Validation Study in the Mediterranean Silvo-Pastoral Ecosystem', Agriculture, 14(8), 1350.

Shi, P., Fu, B., Ninomiya, Y., Sun, J., & Li, Y. 2011, 'Multispectral remote sensing mapping for hydrocarbon seepage-induced lithologic anomalies in the Kuqa foreland basin, south Tian Shan', Journal of Asian Earth Sciences, 46, 70–77.

Warnault, R. 2021, 'Downstream oil theft: Implications and next steps - Atlantic Council', Atlantic Council.

Wekpe, V. O., & Idisi, B. E. 2024, 'Long-Term monitoring of oil spill impacted vegetation in the Niger Delta region of Nigeria: a Google Earth engine derived Vegetation Indices approach', Journal of Geography Environment and Earth Science International, 28(2), 27–40.

Wilton, M. 2021, 'Crop Yield Estimation Using NDVI: A Comparison of Various NDVI Metrics', MSc. Thesis, Department of Agribusiness and Agricultural Economics, University of Manitoba, Winnipeg, Manitoba. Retrieved on 1st December, 2025.

Xue, J., & Su, B. 2017, 'Significant Remote Sensing Vegetation Indices: A Review of Developments and applications', Journal of Sensors, 2017, 1–17.

Zhu, X., Li, Q., & Guo, C. 2024, 'Evaluation of the monitoring capability of various vegetation indices and mainstream satellite band settings for grassland drought', Ecological Informatics, 82, 102717.